34th Annual International Conference of the IEEE EMBS
San Diego, California USA, 28 August - 1 September, 2012

A Fast Adaptive-Gain Orientation Filter of Inertial/Magnetic Data for Human Motion Tracking in Free-living Environments

Ya Tian and Jindong Tan

Abstract— **High-resolution, real-time data obtained by human motion tracking systems can be used for gait analysis, which helps better understanding the cause of many diseases for more effective treatments, such as rehabilitation for outpatients or recovery from lost motor functions after a stroke. This paper presents an analytically derived method for an adaptive-gain complementary filter based on the convergence rate from the Gauss-Newton optimization algorithm (GNA) and the divergence rate from the gyroscope, which is referred as Adaptive-Gain Orientation Filter (AGOF) in this paper. The AGOF has the advantages of one iteration calculation to reduce the computing load and accurate estimation of gyroscope measurement error. Moreover, for handling magnetic distortions especially in indoor environments and movements with excessive acceleration, adaptive measurement vectors and a reference vector for Earth's magnetic field selection schemes are introduced to help the GNA find more accurate direction of gyroscope error. Experimental results are presented to verify the performance of the proposed method, which shows better accuracy of orientation estimation than several well-known methods.**

I. INTRODUCTION

Recent developments in miniature sensor technology have led many researchers to utilize wearable inertial sensors to capture human movement out of controlled volumes, because they are independent from an infrastructure and relatively low cost, light weight and compact in size. Therefore, human limb movements can be measured through the attachment of an inertial/magnetic sensor module in human's free-living environments for the practice of physical medicine and rehabilitation. Such a sensor module typically consists of a tri-axis accelerometer, a tri-axis gyroscope, and a tri-axis magnetometer and is compact in size, which can be called wearable MARG (Magnetic, Angular Rate and Gravity) sensor [1]. Meanwhile, the embedded wireless sensor network (Bluetooth) makes the attachment of sensors much easier.

However, there are two major challenges for estimating orientation using a MARG sensor. First, directly integrating the angular velocity from the tri-axis gyroscope suffers from drift accumulation in a long-term tracking [2], which negatively affects the orientation estimation accuracy. Secondly, as aiding sensors for mitigating the drift, the tri-axis accelerometers and magnetometers are employed for the vertical (Earth's gravity) and the horizontal (Earth's magnetic field) references, respectively. However, accelerometers are sensitive to excessive accelerations under dynamic motion conditions, while magnetometer measurements suffer from local earth magnetic field variations [3], which are easily caused by common everyday objects and influence the direction of the Earth's magnetic field, further affecting the desired orientation estimation.

Y. Tian and J. Tan are with the Department of Mechanical, Aerospace and Biomedical Engineering, The University of Tennessee, Knoxville, TN 37996, USA. e-mail: {ytian3, tan}@utk.edu.

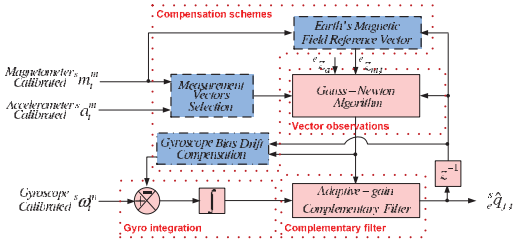

Fig. 1. The main framework of the AGOF for orientation estimation.

In order to overcome these challenges, an Adaptive-Gain Orientation Filter (AGOF) is proposed in this paper based on the basic theory of deterministic approach and frequency-based approach, and it is tested on a newly developed MARG sensor. The main framework of the proposed AGOF (Adaptive-Gain Orientation Filter) includes 4 major parts: (a) gyro integration; (b) vector observations; (c) complementary filter; and (d) compensation schemes, which are shown as dotted blocks in Figure 1. The main contributions of this paper are summarized as follows: 1) an analytical approach of combining the GNA with a complementary filter for faster quaternion updates; 2) adaptive measurement vectors and a reference vector for Earth's magnetic field selection schemes in conjunction with the GNA; 3) a gyroscope bias drift compensation scheme for one input of the complementary filter; and 4) an adaptive-gain complementary filter based on the convergence rate from the GNA and the divergence rate from the gyroscope.

II. ADAPTIVE-GAIN ORIENTATION FILTER

For brevity and clarity, the quaternion-based orientation representation is chosen and the definitions of mathematical variables are firstly described as: s–indicating the sensor frame, e–indicating the earth frame, g–gravity vector, ${}^s a$–measurements from the accelerometer in s, ${}^s\omega$–measurements from the gyroscope in s, ${}^s m$–measurements from the magnetometer in s, ${}^s_e q_t$–quaternion-based orientation from s to e at time t, ${}^s_e\hat{q}_{\omega,t}$–orientation estimated from the gyroscope at time t, ${}^s_e\hat{q}_{a,t}$–orientation estimated from the accelerometer and magnetometer at time t, and ${}^s_e\hat{q}_{f,t}$–orientation estimated from the complementary filter fusion at time t.

A. Orientation Estimation from Gyroscope

The tri-axis gyroscope measures the angular velocities ${}^s\omega$, which is expressed in s and represented as a four-element row vector: ${}^s\omega = [0\ \omega_x\ \omega_y\ \omega_z]$ using the quaternion representation. The quaternion derivation ${}^s_e\dot{q}$ describing the rate of change of orientation from s to e can be calculated as:

$$ {}^s_e\dot{q} = \frac{1}{2}{}^s_e\hat{q} \otimes {}^s\omega = \frac{1}{2}\Omega({}^s\omega){}^s_e\hat{q} \quad (1) $$

where $\Omega({}^s\omega)$ is the 4×4 skew-symetric matrix of a quaternion ${}^s\omega = [0\ \omega_x\ \omega_y\ \omega_z]$.

Therefore the orientation from s to e at time $t+\Delta t$, ${}^s_e q_{\omega,t+\Delta t}$, can be calculated by integrating the quaternion time derivation ${}^s_e\dot{q}_{\omega,t+\Delta t}$ as described by (2) with known initial condition ${}^s_e\hat{q}_{\omega,t}$. Here, the sub-script ω denotes that the orientation based on quaternion representation is obtained from the gyroscope readings.

$$\begin{array}{rcl} {}^s_e\dot{q}_{\omega,t+\Delta t} & = & \frac{1}{2}{}^s_e\hat{q}_{\omega,t}\otimes{}^s\omega_{t+\Delta t} \\ {}^s_e q_{\omega,t+\Delta t} & = & {}^s_e\hat{q}_{\omega,t}+{}^s_e\dot{q}_{\omega,t+\Delta t}\Delta t \end{array} \tag{2}$$

where Δt is the sampling time and ${}^s_e\hat{q}_{\omega,t}$ is the previous orientation estimation represented by unit quaternion, which can also be obtained by using iterative equations (2).

B. Fast Gauss-Newton Algorithm for Vector Observations

1) Problem Description: Since the accelerometer and magnetometer can measure the absolute orientation against the earth, the orientation from their measurements could be computed using a fast convergence approach called the Gauss-Newton optimization algorithm (GNA). Given their normalized reference directions in the earth frame (${}^e z_a = [0\ 0\ 0\ 1]$ for the accelerometer and ${}^e z_{m,t} = [0\ \tilde{m}_x\ \tilde{m}_y\ \tilde{m}_z]$ for the magnetometer) and their normalized measurements shown in (3), the problem for finding the unit quaternion ${}^s_e\hat{q}_t$ based on

$$\begin{array}{rcl} {}^sA_t & = & \dfrac{{}^s a_t^m}{\|{}^s a_t^m\|} \quad = \quad [0\ a_{x,t}\ a_{y,t}\ a_{z,t}] \\ {}^sM_t & = & \dfrac{{}^s m_t^m}{\|{}^s m_t^m\|} \quad = \quad [0\ m_{x,t}\ m_{y,t}\ m_{z,t}] \end{array} \tag{3}$$

the GNA can be modeled as follows:

$$\begin{array}{rl} find: & {}^s_e\hat{q}_t = [\hat{q}_0\ \hat{q}_x\ \hat{q}_y\ \hat{q}_z] \\ minimize: & f({}^s_e\hat{q}_t) = \frac{1}{2}\varepsilon({}^s_e\hat{q}_t)^T\varepsilon({}^s_e\hat{q}_t) \\ where: & \varepsilon = \begin{cases} \varepsilon_a({}^s_e\hat{q}_t) = {}^s_e\hat{q}_t\otimes{}^e z_a\otimes{}^s_e\hat{q}_t^* - {}^sA_t \\ \varepsilon_m({}^s_e\hat{q}_t) = {}^s_e\hat{q}_t\otimes{}^e z_{m,t}\otimes{}^s_e\hat{q}_t^* - {}^sM_t \end{cases} \\ subject\ to: & {}^s_e\hat{q}_t\in\mathbb{R}^4 \ \ and \ \ {}^s_e\hat{q}_t{}^s_e\hat{q}_t^T = \|{}^s_e\hat{q}_t\|^2 = 1 \end{array}$$

where f is the cost function, defined as the square of the error function $\varepsilon = [\varepsilon_a \quad \varepsilon_m]^T$ which combines ε_a from the accelerometer and ε_m from the magnetometer together. It can be represented as follows:

$$\varepsilon({}^s_e\hat{q}_t) = \begin{bmatrix} 2(\hat{q}_x\hat{q}_z-\hat{q}_0\hat{q}_y)-a_{x,t} \\ 2(\hat{q}_0\hat{q}_x+\hat{q}_y\hat{q}_z)-a_{y,t} \\ 2(0.5-\hat{q}_x^2-\hat{q}_y^2)-a_{z,t} \\ 2\tilde{m}_x(0.5-\hat{q}_y^2-\hat{q}_z^2)+2\tilde{m}_y(\hat{q}_0\hat{q}_z+\hat{q}_x\hat{q}_y)+2\tilde{m}_z(\hat{q}_x\hat{q}_z-\hat{q}_0\hat{q}_y)-m_{x,t} \\ 2\tilde{m}_x(\hat{q}_x\hat{q}_y-\hat{q}_0\hat{q}_z)+2\tilde{m}_y(0.5-\hat{q}_x^2-\hat{q}_z^2)+2\tilde{m}_z(\hat{q}_0\hat{q}_x+\hat{q}_y\hat{q}_z)-m_{y,t} \\ 2\tilde{m}_x(\hat{q}_0\hat{q}_y+\hat{q}_x\hat{q}_z)+2\tilde{m}_y(\hat{q}_y\hat{q}_z-\hat{q}_0\hat{q}_x)+2\tilde{m}_z(0.5-\hat{q}_x^2-\hat{q}_y^2)-m_{z,t} \end{bmatrix}$$

2) Fast Gauss-Newton Algorithm: According to the above-mentioned formulated problem, the conventional GNA consists of the following optimization steps:

$$\begin{array}{l} {}^s_e q(k+1) \\ = {}^s_e\hat{q}(k) - (J(k)^TJ(k))^{-1}J(k)^T\varepsilon({}^s_e\hat{q}(k)) \\ \qquad (k = 0,1,2,\cdots,n) \end{array} \tag{4}$$

where k is an iteration number and $J(k)$ is the Jacobian of ε. Actually, (4) can be rewritten as shown in (5).

$$\begin{array}{l} {}^s_e\hat{q}(n+1) \\ = {}^s_e\hat{q}(0) - \sum_{k=0}^{n}(J(k)^TJ(k))^{-1}J(k)^T\varepsilon({}^s_e\hat{q}(k)) \\ = {}^s_e\hat{q}(0) - \lambda_k(J(0)^TJ(0))^{-1}J(0)^T\varepsilon({}^s_e\hat{q}(0)) \end{array} \tag{5}$$

${}^s_e\hat{q}(n+1)$ is actually the final optimal orientation at time $t+\Delta t$, denoted by ${}^s_e\hat{q}_{a,t+\Delta t}$ and ${}^s_e\hat{q}(0)$ is the previous orientation estimation at time t, denoted by ${}^s_e\hat{q}_{f,t}$. λ_k will change with every iteration to an optimal value. In fact, it is acceptable to compute one iteration per time period as long as $\lambda_{t+\Delta t}$, which guarantees the convergence rate of ${}^s_e\hat{q}_{a,t+\Delta t}$, is restricted to the physical orientation rate ${}^s_e\dot{q}_{\omega,t+\Delta t}$ from the gyroscope as this avoids overshooting due to an unnecessary large step size. Therefore, (5) can be simplified as (6) with only one iteration and an optimal value of $\lambda_{t+\Delta t}$ can be calculated as equation (7), which is defined the same as μ_t in [4].

$$\begin{array}{l} {}^s_e\hat{q}_{a,t+\Delta t} = {}^s_e\hat{q}_{f,t} - \\ \lambda_{t+\Delta t}(J({}^s_e\hat{q}_{f,t})^TJ({}^s_e\hat{q}_{f,t}))^{-1}J({}^s_e\hat{q}_{f,t})^T\varepsilon({}^s_e\hat{q}_{f,t}) \end{array} \tag{6}$$

$$\begin{array}{l} = {}^s_e\hat{q}_{f,t} - \lambda_{t+\Delta t}\dfrac{\Delta\hat{q}}{\|\Delta\hat{q}\|} \\ \lambda_{t+\Delta t} = \alpha\|{}^s_e\dot{q}_{\omega,t+\Delta t}\|\Delta t,\ \alpha>1 \end{array} \tag{7}$$

where α is an augmentation of λ to account for noise in the accelerometer and magnetometer.

C. Adaptive-Gain Complementary Filter

As described in [5], a complementary filter is mainly designed for two noise sources with complementary spectral characteristics, so the idea is to pass the accelerometer and magnetometer signals through a low-pass filter and the gyroscope signals through a high-pass filter and combine them to give the final rate. The proposed filter combines the advantage of the complementary filter and kalman filter, where time-variant parameters k_t and $(1-k_t)$ are set as the weights of each orientation for more robust results compared with the convention complementary filter, denoted as (8). The gain k_t is adaptively adjusted by using the convergence rate $\frac{\lambda_t}{\Delta t}$ of low-frequency ${}^s_e\hat{q}_{a,t}$ from vector observations based on the GNA and the divergence rate β of high-frequency ${}^s_e\hat{q}_{\omega,t}$ from the gyroscope, shown as group 3 in Figure 2.

$${}^s_e\hat{q}_{f,t} = k_t{}^s_e\hat{q}_{a,t} + (1-k_t){}^s_e\hat{q}_{\omega,t},\ 0\le k_t\le 1 \tag{8}$$

Based on the same concept proposed in [4], the final orientation estimation can be obtained using (9).

$$\begin{array}{c} {}^s_e\hat{q}_{f,t+\Delta t} = {}^s_e\hat{q}_{f,t} + {}^s_e\dot{q}_{f,t+\Delta t}\Delta t \\ {}^s_e\dot{q}_{f,t+\Delta t} = {}^s_e\dot{q}_{\omega,t+\Delta t} - \beta{}^s_e\dot{q}_{\varepsilon,t+\Delta t} \\ {}^s_e\dot{q}_{\varepsilon,t+\Delta t} = \dfrac{\Delta\hat{q}}{\|\Delta\hat{q}\|} \end{array} \tag{9}$$

where ${}^s_e\dot{q}_{f,t+\Delta t}$ is the estimated orientation rate, which can be calculated as the rate of change of orientation measured by the gyroscope, ${}^s_e\dot{q}_{\omega,t+\Delta t}$, with the magnitude of the gyroscope measurement error (usually zero-mean error), β, removed in the direction of the estimated error, $\dot{q}_\varepsilon$, computed from accelerometer and magnetometer measurements. β can be obtained using the method in [4].

D. Compensation Schemes

1) Gyroscope Bias Drift Compensation: With the disadvantage of accumulated drift over long-time tracking, ${}^s_e\dot{q}_\varepsilon$ is also used for the gyroscope bias drift compensation derived as the inverse to the relationship defined in (1). So the angular error ${}^s\omega_e$, angular bias ${}^s\omega_b$, and angular velocity ${}^s\omega_c$ after compensation in each gyroscope axis can be expressed in (10) by using the normalized direction of $\dot{q}_\varepsilon$, shown as Group 2 in Figure 2.

$$\begin{array}{c} {}^s\omega_{e,t+\Delta t} = 2{}^s_e\hat{q}^*_{f,t+\Delta t}\otimes{}^s_e\dot{q}_{\varepsilon,t+\Delta t} \\ {}^s\omega_{b,t+\Delta t} = \zeta\sum_{t+\Delta t}{}^s\omega_{e,t+\Delta t}\Delta t \\ {}^s\omega_{c,t+\Delta t} = {}^s\omega_{t+\Delta t} - {}^s\omega_{b,t+\Delta t} \end{array} \tag{10}$$

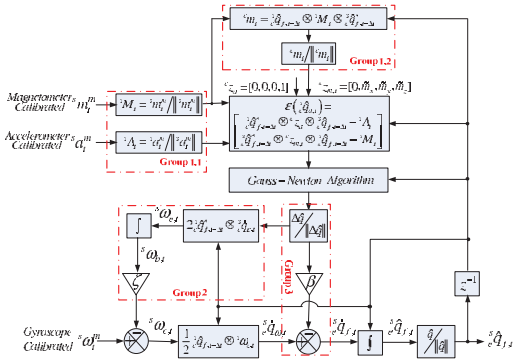

Fig. 2. The block diagram of the AGOF design for MARG sensors.

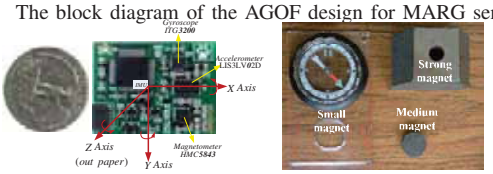

(a) The top view and its frame (b) Illustration of Test I

Fig. 3. Prototype design for MARG sensor and experimental illustration.

where ζ accounts for the rate of convergence to remove non-zero-mean gyroscope measurement errors, which can be similarly determined as β.

2) Accelerometer and Magnetometer Compensation: In order to select the best reliable vectors among the sensor measurements as inputs to the filter, accelerometer and magnetometer measurements should be compensated, especially within fast motion and temporary magnetic disturbances. The input vectors ${}^sA$ and ${}^sM$ for the GNA can be compensated using the following criteria, which are similarly used in [6], but more robust with the adaptive reference vector selection for Earth's magnetic field, are implemented in this paper.

$$
\begin{aligned}
{}^sA_t &= \begin{cases} \dfrac{{}^sa_t^m}{\|{}^sa_t^m\|}, & \text{if } |\|{}^sa_t^m\| - \|g\|| \le \varepsilon_a \\ {}^s_e\hat{q}^*_{t-\Delta t} \otimes {}^e z_a \otimes {}^s_e\hat{q}_{t-\Delta t}, & \text{otherwise} \end{cases} \\
{}^e z_{m,t} &= \begin{cases} \dfrac{{}^sm_{t=0}^m}{\|{}^sm_{t=0}^m\|}, & \text{if } |\|{}^sm_t^m\| - \|m_{t=0}\|| \le \varepsilon_m \\ {}^s_e\hat{q}_{t-\Delta t} \otimes {}^sM_{t-\Delta t} \otimes {}^s_e\hat{q}^*_{t-\Delta t}, & \text{otherwise} \end{cases} \\
{}^sM_t &= \begin{cases} \dfrac{{}^sm_t^m}{\|{}^sm_t^m\|}, & \text{if } |\|{}^sm_t^m\| - \|m_{t=0}\|| \le \varepsilon_m \\ {}^s_e\hat{q}^*_t \otimes {}^e z_{m,t} \otimes {}^s_e\hat{q}_t, & \text{otherwise} \end{cases}
\end{aligned}
$$

III. EXPERIMENTAL VALIDATION AND RESULTS

A. Experimental Validation

To verify the proposed algorithm, a newly small MARG platform is developed shown in Figure 3(a). The RMS (Root Mean Square) is chosen as the criterion to evaluate the accuracy of the proposed AGOF method. A Vicon system [7] was used as ground truth, and three other well-known algorithms were used to compare with the proposed AGOF, which include the KF(Kalman-based Filter), FQA (Factored Quaternion Algorithm) proposed in [8], and GDA (Gradient Descent Algorithm) proposed in [4]. The magnetic distortion, which will affect not only the magnitude but also the orientation of the magnetic field, can be generated by swaying a magnetic iron, shown in Figure 3(b). The filter gains for the complementary filter, and the threshold values in the vector selections were set as: $\beta = 0.0756$, $\zeta = 0.003$, $\varepsilon_a = 0.25 m/s^2$, and $\varepsilon_m = 0.02 Guass$.

TABLE I

STATIC AND DYNAMIC ACCURACY OF METHODS FROM THE AGOF, KF, GDA AND FQA (MD:MAGNETIC DISTORTION).

Euler angles \ Methods	AGOF	KF	GDA	FQA
RMS[Roll] Static without MD :	0.2316°	0.7890°	0.5811°	1.2311°
RMS[Roll] Static with MD:	0.2910°	8.2316°	9.1831°	9.4256°
RMS[Roll] Dynamic:	0.6645°	3.8695°	2.8252°	12.5791°
RMS[Pitch] Static without MD :	0.2664°	0.8191°	0.5023°	1.3813°
RMS[Pitch] Static with MD:	0.2742°	8.5142°	9.2472°	9.0811°
RMS[Pitch] Dynamic:	0.6018°	3.3471°	2.6680°	13.2781°
RMS[Yaw] Static without MD :	0.5322°	1.1572°	1.0734°	1.5193°
RMS[Yaw] Static with MD:	0.9496°	11.1532°	10.5811°	20.8124°
RMS[Yaw] Dynamic:	0.8182°	8.5451°	10.1101°	15.1125°
Real-time Tracking	Yes	No	Yes	No
Gyro Drift Compensation	Yes	No	Yes	No
MD Compensation	Yes	No	Yes	No
Accelerometer Compensation	Yes	No	No	No

B. Experimental Results

1) Test I: No Movement with Magnetic Disturbances: In this test scenario, the sensor arrays kept still and a magnetic shown in Figure 3(b) was swayed around the sensor intermittently. The magnetic disturbances for 3 axes were clearly shown in Figure 5(f), marked in the red area. Figure 5(a) shows the Euler angles which were calculated from the GDA(black dash-dotted), KF(purple dotted), FQA(green line), and AGOF(blue dashed).

2) Test II: Slow Movement within a Magnetically Homogeneous Environment: This test involved three typical motions (single roll, pitch and yaw movements) and the results from the Vicon system were used as the ground truth to test the accuracy of the proposed method. Figure 4 shows the measured and estimated angles in upper plot and estimated errors in lower plot.

3) Test III: Sudden Fast Movement within a Magnetically Homogeneous Environment: In Test III, the MARG sensor went through a sudden acceleration[see Figure 5(e) in red area]. Figure 5(b) shows that the proposed AGOF offered more accurate estimation than the GDA , KF, and FQA.

4) Gyroscope Bias Drift Estimation with Magnetic Disturbances for Test I: Figure 5(c) shows the estimated bias results for three axes of the gyroscope using the proposed AGOF and the GDA proposed by Madgwick within magnetic disturbances, plotted against the actual gyroscope measurements.

5) Static and Dynamic Accuracy: The static and dynamic RMS error values of Euler angles were calculated based on Test I, II and III to test the accuracy of the proposed AGOF, KF, GNA, and FQA. For the static accuracy, it was evaluated with and without magnetic distortion. Table I shows three Euler angles' RMS errors of static and dynamic movements from four methods.

6) Real-time Orientation Visualization and Motion Capture of Human Upper Limb: Figure 6(a) shows a 3D coordinate system (Red-X axis, Green-Y axis and Blue-Z axis) demonstration of real-time orientation tracking estimated by the newly developed MARG sensor. The 3D visualization is illustrated on the user PC by using the OpenGL. Figure 6(b) shows the real pose of the upper limb and the visualization of its estimation by MARG sensors.

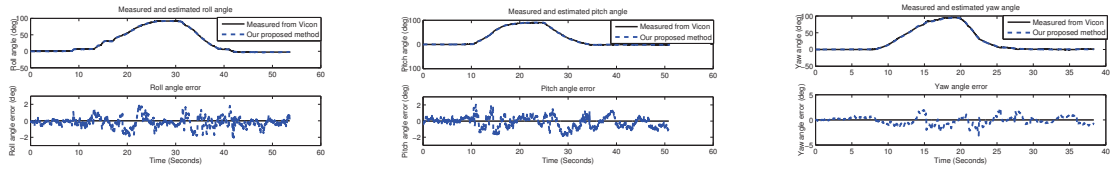

(a) Roll angle (b) Pitch angle (c) Yaw angle

Fig. 4. Results for measured and estimated angle (top) and error (bottom).

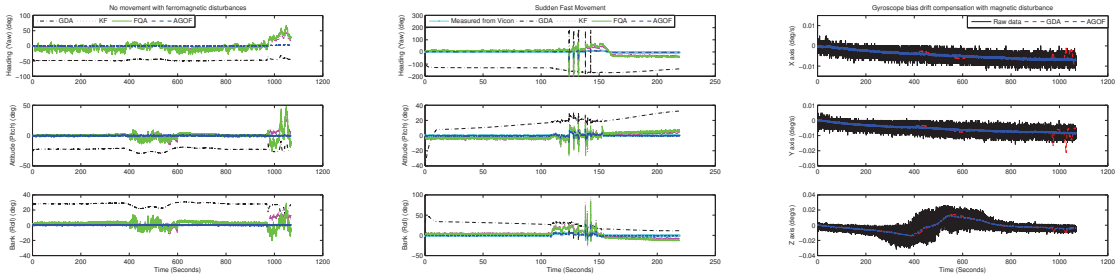

(a) Results for magnetic disturbances (b) Results for sudden fast movement (c) Results for Gyro bias

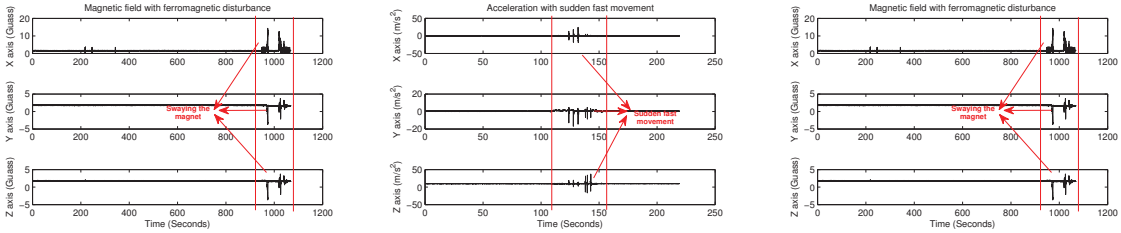

(d) Distorted magnetic field (e) Acceleration data (f) Distorted magnetic field

Fig. 5. Results for Test I, III and Gyro bias using the proposed AGOF compared with the GDA, KF, and FQA.

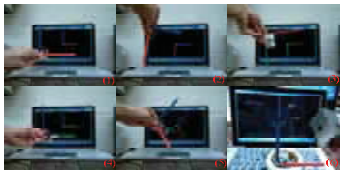

(a) Real-time visualization

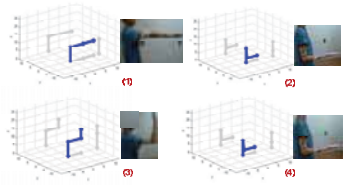

(b) Motion capture

Fig. 6. (a)The real-time 3D orientation visualization of MARG sensor: (1)initial position; (2)rotating around Y axis; (3)rotating around X axis; (4)rotating around Z axis; (5)Random rotating around X, Y and Z axis together; (6)static demonstration with strong magnetic distortion.(b)Motion capture of human upper limb. On the right side of each photograph: a user wearing the MARG sensors is moving his upper limb. On the left side: the real-time reconstruction of the movements and shadows of human upper limb in each plane.

IV. Conclusion

This paper presented an adaptive-gain orientation filter (AGOF) with adaptive vector selections designed for real-time human motion tracking in free-living environments. In particular, the proposed method is effective at handling severe magnetic distortion and high dynamic movement with the compensation schemes for each sensor. The RMS error of the estimated orientation is less than two degrees. Due to its high computational efficiency and accuracy, the proposed algorithm can be potentially implemented in a network of miniature MARG sensors for human body movement, forming a truly portable and ambulatory motion tracking system. This paper demonstrated the human-upper-limb-motion-capture using the proposed method, and the results also illustrated the high accuracy.

References

[1] X. Yun, M. Lizarraga, E. R. Bachmann, and R. B. McGhee, "An improved quaternion-based kalman filter for real-time tracking of rigid body orientation," *Proceedings of the IEEE/RSJ International Conference on Intelligent Robots and Systems*, vol. 2, pp. 1074–1079, 2003.

[2] F. Mohd-Yasin, D. J. Nagel, and C. E. Korman, "Noise in MEMS," *Measurement Science and Technology*, vol. 21, no. 1, p. 012001, 2010.

[3] E. R. Bachmann, X. Yun, and A. Brumfield, "Limitations of attitude estimation algorithms for inertial/magnetic sensor modules," *IEEE Robotics & Automation Magazine*, vol. 14, no. 3, pp. 76–87, 2007.

[4] S. O. H. Madgwick, A. J. L. Harrison, and R. Vaidyanathan, "Estimation of imu and marg orientation using a gradient descent algorithm," *Proceedings of the IEEE International Conference on Rehabilitation Robotics*, vol. 51, no. 2, pp. 1–7, 2011.

[5] E. R. Bachmann, *Inertial and magnetic tracking of limb segment orientation for inserting humans into synthetic environments*. PhD thesis, Naval Postgraduate School, 2000.

[6] J. K. Lee and E. J. Park, "A fast quaternion-based orientation optimizer via virtual rotation for human motion tracking," *IEEE Transactions on Biomedical Engineering*, vol. 56, no. 5, pp. 1574–1582, 2009.

[7] "Vicon motion capture systems —- http://www.vicon.com,"

[8] X. Yun, E. R. Bachmann, and R. B. McGhee, "A simplified quaternion-based algorithm for orientation estimation from earth gravity and magnetic field measurements," *IEEE Transactions on Instrumentation and Measurement*, vol. 57, no. 3, pp. 638–650, 2008.